Production of the newly observed $\bar{T}_{c\bar{s}0}$ by kaon-induced reactions on a proton or neutron target

Yin Huang* and Hao Hei
School of Physical Science and Technology, Southwest Jiaotong University, Chengdu 610031, China

Jing-wen Feng
School of Physics and Electronic Engineering, Sichuan Normal University, Chengdu 610101, China

Xurong Chen
Institute of Modern Physics, Chinese Academy of Sciences, Lanzhou 730000, China
and School of Nuclear Science and Technology, University of Chinese Academy of Sciences, Beijing 100049, China

Rong Wang
Institute of Modern Physics, Chinese Academy of Sciences, Lanzhou 730000, China

(Received 28 August 2023; accepted 4 October 2023; published 26 October 2023)

Recently, a new doubly charged tetraquark $T^a_{c\bar{s}0}(2900)^{++}$ and its neutral partner $T^a_{c\bar{s}0}(2900)^0$ at the invariant mass spectrum of πD_s were observed by the LHCb Collaboration. According to its properties, such as the mass and decay width, $T^a_{c\bar{s}0}(2900)^{++/0}$ has been suggested to be a compact multiquark state or a hadron molecule. In order to distinguish the various interpretations of $T^a_{c\bar{s}0}(2900)^{++/0}$, we investigate the possibility of studying $\bar{T}^a_{c\bar{s}0}(2900)$ [the antiparticle of $T^a_{c\bar{s}0}(2900)$] by kaon-induced reactions on a proton target in an effective Lagrangian approach. The production mechanism is characterized by the t-channel D-meson exchange. Our theoretical approach is based on the assumption that $\bar{T}^a_{c\bar{s}0}(2900)$ can be either a K^*D^*-$D_s^*\rho$ molecule or a compact tetraquark state. Using the coupling constants of $\bar{T}^a_{c\bar{s}0}(2900)$ to the KD channel obtained from the molecule or compact tetraquark picture of $\bar{T}^a_{c\bar{s}0}(2900)$, we compute the cross sections for the process $K^-n \to \bar{T}^a_{c\bar{s}0}(2900)^{--}\Lambda_c^+$. The $\bar{K}N$ initial-state interaction mediated by Pomeron and Reggeon exchanges is also included, which reduces the production of $\bar{T}^a_{c\bar{s}0}(2900)$. Our calculations show that whether $\bar{T}^a_{c\bar{s}0}(2900)$ is a molecule or a compact tetraquark state, the cross sections for the $K^-n \to \bar{T}^a_{c\bar{s}0}(2900)^{--}\Lambda_c^+$ reaction are of similar magnitude, ranging from approximately 0.150 nb to 0.540 nb. However, a clearer comparison can be made by computing the cross section of the $K^-n \to \bar{T}^a_{c\bar{s}0}(2900)^{--}\Lambda_c^+ \to \pi^- D_s^- \Lambda_c^+$ reaction. The results indicate that the cross section for the molecule assignment of $\bar{T}^a_{c\bar{s}0}(2900)$ can reach up to 3.66×10^{-3} nb, which is significantly smaller than that of 0.244 nb, by assuming $\bar{T}^a_{c\bar{s}0}(2900)$ as a compact tetraquark state. These results can be measured in future experiments, and they can be used to test the nature of $\bar{T}^a_{c\bar{s}0}(2900)$. Lastly, we also propose to search for the unreported charged tetraquark $T^a_{c\bar{s}0}(2900)^+$ in the $K^-p \to \bar{T}^a_{c\bar{s}0}(2900)^-\Lambda_c^+$ reaction.

DOI: 10.1103/PhysRevD.108.076019

I. INTRODUCTION

Studying hadrons with more complex internal structures than quark states, where mesons are composed of quark-antiquark pairs [1], and baryons are constructed from three quarks [2,3], is a prominent topic in particle physics. We call them exotic hadrons. For an extended period, little noteworthy advancement has been made in the exploration of exotic states—only a few phenomena suggesting that quarks $u/d/s$ can form exotic hadrons. For example, in constituent quark models, the mass of the strange quark is approximately 50% heavier than that of the u/d quarks. This leads to questions regarding why the $\Lambda(1405)$ has a significantly lower mass than the $N(1535)$. Moreover, it is puzzling to observe that the $N(1440)$, as a

*huangy2019@swjtu.edu.cn

$N = 2$ baryon, is much lighter than the nucleon resonance $N(1535)$ with $N = 1$, where N is the main quantum number. These issues led Zou and his collaborators to propose the existence of significant five-quark components in the nucleon and its resonances [4–6]. The mass inversion problem could be easily understood if there are substantial five-quark $uuds\bar{s}$ components in the $N(1535)$ [7,8]. Furthermore, the five-quark configurations also provide a natural explanation for its large strange decay [9,10].

However, it was in 2003, when the Belle Collaboration observed the $X(3872)$ in the $\pi^+\pi^- J/\psi$ mass spectra [11], that this field entered a new era. From its observed decay mode, $X(3872)$ is known to consist of a pair of hidden-charm quarks and two pairs of light quarks. Subsequent discoveries of several hidden-charm pentaquark states, including $P_c(4380)$, $P_c(4440)$, $P_c(4457)$, $P_c(4312)$, $P_{cs}(4338)$, and $P_{cs}(4459)$, have further strengthened the belief in significant progress in the research of exotic hadrons [12–17]. The recent observation of a doubly charged tetraquark and its neutral partner by the LHCb Collaboration in the analysis of the $B^0 \to \bar{D}^0 D_s^+ \pi^-$ and $B^- \to \bar{D}^- D_s^+ \pi^-$ reactions [18] marks another significant advancement in the study of exotic hadrons. Their masses and widths were measured to be

$$\begin{aligned} T^a_{c\bar{s}0}(2900)^0: \quad & M = 2.892 \pm 0.014 \pm 0.015 \text{ GeV}, \\ & \Gamma = 0.119 \pm 0.026 \pm 0.013 \text{ GeV}, \\ T^a_{c\bar{s}0}(2900)^{++}: \quad & M = 2.921 \pm 0.017 \pm 0.020 \text{ GeV}, \\ & \Gamma = 0.137 \pm 0.032 \pm 0.017 \text{ GeV}, \end{aligned} \tag{1}$$

respectively. Supposing the states belong to the same isospin triplet, the experiment also gave the shared mass and width,

$$T_{c\bar{s}0}: M = 2908 \pm 23 \text{ MeV}, \qquad \Gamma = 136 \pm 25 \text{ MeV}. \tag{2}$$

It is worth noting that the existence of such a tetraquark state had been predicted in the DK-$D_s^*\rho$ interaction before its experimental discovery [19].

Similarly to the challenges faced with other exotic hadrons, the true internal structure of these two newly observed mesons cannot be completely determined based on existing experimental data. Due to the close proximity of the mass of $T^a_{c\bar{s}0}(2900)$ to the DK threshold, the authors of Ref. [20] proposed a novel interpretation for the recently discovered $T^a_{c\bar{s}0}(2900)$. They suggest that these two states could be an isovector D^*K^* molecular state with quantum numbers $I(J^P) = 1(0^+)$. In an independent study conducted by the authors of Ref. [21], it was found that if the $T^a_{c\bar{s}0}(2900)^0$ is indeed a molecular state formed by $D^{*0}K^{*0}$, its primary decay mode would likely be into D^0K^0, rather than the observed experimental decay channel $D_s^+\pi^-$. The authors in Ref. [22] support the $T^a_{c\bar{s}0}(2900)$ as a D^*K^* molecule based on the analysis of the mass spectrum and the partial widths using the QCD light-cone sum rule approach and soft-meson approximation. The mass of the $T^a_{c\bar{s}0}$ was studied in the coupled-channel approach, and it was shown that $T_{c\bar{s}0}$ might be a D^*K^*-$D_s^*\rho$ couple molecular state [23]. However, Ref. [24] reached a strikingly different conclusion, arguing that $T^a_{c\bar{s}0}$ should not be considered as a D^*K^* bound state, but instead might be made up of compact tetraquarks.

Indeed, the newly observed two mesons can be assigned to be the lowest $1S$-wave tetraquark states [25] within the framework of a nonrelativistic potential quark model. Their analysis indicates that the dominant decay mode is the $D_s^*\rho$. Furthermore, the compact tetraquark explanation of $T^a_{c\bar{s}0}$ is also supported by estimates obtained from the multiquark color flux-tube model [26]. QCD sum rules, informed by the examination of the mass spectrum and the two-body strong decays, have led Refs. [27,28] to classify $T^a_{c\bar{s}0}$ as compact tetraquark states. The studies also reveal that the primary decay modes for $T^a_{c\bar{s}0}$ involve $D_s\pi$ and DK channels [28]. The compact tetraquark candidates for $T^a_{c\bar{s}0}$ gain additional support from Refs. [29–31]. We note that $T_{c\bar{s}}(2900)$ can be interpreted as a threshold effect from the interaction between the D^*K^* and $D_s^*\rho$ channels [32]. In addition, the kinetic effect from a triangle singularity for $T^a_{c\bar{s}0}$ is also proposed in Ref. [33].

In addition to analyzing the mass spectrum and decay width, exploring the production mechanism provides a more effective approach to evaluating the nature of $T^a_{c\bar{s}0}$. This is mainly due to the production process's strong dependence on the internal structure of $T^a_{c\bar{s}0}$. We find that whether $T^a_{c\bar{s}0}$ is a molecular state or a compact multiquark state, it exhibits a significant KD decay width. This motivates our quest to search for $\bar{T}^a_{c\bar{s}0}(2900)^{--}$ in the $K^- n \to \bar{T}^a_{c\bar{s}0}(2900)^{--}\Lambda_c^+$ and $K^- n \to \bar{T}^a_{c\bar{s}0}(2900)^{--}\Lambda_c^+ \to \pi^- D_s^- \Lambda_c^+$ reactions. Notably, high-energy kaon beams are available at OKA@U-70 [34], SPS@CERN [35], CERN/AMBER [36], and potential upgrades to the J-PARC kaon beam, enabling us to reach the necessary energy range for $\bar{T}^a_{c\bar{s}0}(2900)^{--}$ production [37]. Consequently, searching for $\bar{T}^a_{c\bar{s}0}(2900)^{--}$ in the $K^- n \to \bar{T}^a_{c\bar{s}0}(2900)^{--}\Lambda_c^+$ and $K^- n \to \bar{T}^a_{c\bar{s}0}(2900)^{--}\Lambda_c^+ \to \pi^- D_s^- \Lambda_c^+$ reactions becomes feasible. This approach facilitates a straightforward differentiation between molecular and compact tetraquark states through the production process.

In this study, we examine the recently observed $\bar{T}^a_{c\bar{s}0}(2900)$ production in the $K^- n \to \bar{T}^a_{c\bar{s}0}(2900)^{--}\Lambda_c^+$ and $K^- n \to \bar{T}^a_{c\bar{s}0}(2900)^{--}\Lambda_c^+ \to \pi^- D_s^- \Lambda_c^+$ reactions by considering $T^a_{c\bar{s}0}$ as a molecular state and as a compact multiquark state, respectively. A conclusive determination of the inner structure of $T^a_{c\bar{s}0}$ can be attained by comparing the obtained cross section with future experimental data. To enhance the reliability of our predictions, the effect from the

$\bar{K}N$ initial-state interaction (ISI) must be taken into account due to the existence of plenty of experimental information about the $\bar{K}N$ elastic interaction in the considered energy region. Moreover, we also propose to search for its isospin partner $\bar{T}^a_{c\bar{s}0}(2900)^-$ in the $K^- p \to \bar{T}^a_{c\bar{s}0}(2900)^- \Lambda_c^+$ reaction. This paper is organized as follows: In Sec. II, we present the theoretical formalism. In Sec. III, the numerical result is given, followed by discussions and conclusions in the last section.

II. FORMALISM AND INGREDIENTS

In this study, we investigate the feasibility of measuring $\bar{T}^a_{c\bar{s}0}(2900)^{--}$ in the $K^- n \to \bar{T}^a_{c\bar{s}0}(2900)^{--}\Lambda_c^+$ reaction. We consider two scenarios for $T^a_{c\bar{s}0}$: one as a molecular state, and the other as a compact multiquark state. The considered Feynman diagrams are illustrated in Fig. 1, which includes only the t-channel D^--meson exchange diagram. The ISI is represented by the red circle. This production process differs from the complex proton-proton collisions [18], as $\bar{T}^a_{c\bar{s}0}(2900)^{--}$ production in $K^- n \to \bar{T}^a_{c\bar{s}0}(2900)^{--}\Lambda_c^+$ occurs more simply. The reason lies in the significantly lower required center-of-mass energies compared to proton-proton collisions. At these lower energies, we can neglect contributions from the s and u channels, which involve the creation of an additional $c\bar{c}$ quark pair in kaon-induced production and are typically strongly suppressed. Hence, the $K^- n \to \bar{T}^a_{c\bar{s}0}(2900)^{--}\Lambda_c^+$ reaction is expected to be primarily governed by Born terms through the t-channel D^- exchanges, resulting in minimal background interference.

To calculate the diagrams depicted in Fig. 1, it is necessary to determine the effective Lagrangian densities corresponding to the relevant interaction vertices. In the case of $\Lambda_c ND$ coupling, we adopt the Lagrangian densities employed in Refs. [38,39]:

$$\mathcal{L}_{\Lambda_c ND} = i g_{\Lambda_c ND} \bar{\Lambda}_c \gamma_5 N D + \text{H.c.}, \tag{3}$$

where the coupling constant $g_{\Lambda_c ND} = -13.98$ is established from the SU(4) invariant Lagrangians [40] in terms of $g_{\pi NN} = 13.45$ and $g_{\rho NN} = 6.0$. N, D, and Λ_c are the nucleon, D-meson, and Λ_c^+-baryon fields, respectively.

To calculate the diagrams depicted in Fig. 1, it is also necessary to determine the effective Lagrangian densities

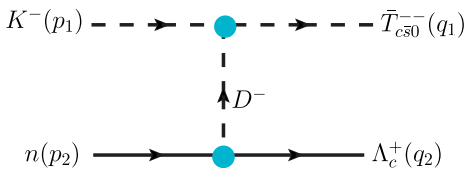

FIG. 1. Feynman diagram for the $K^- n \to \bar{T}^a_{c\bar{s}0}(2900)^{--}\Lambda_c^+$ reaction: the contributions from the t-channel D^--meson exchange. We also show the definition of the kinematics (p_1, p_2, q_1, q_2) that we use in the present calculation.

for the interaction vertex involving $\bar{T}^a_{c\bar{s}0}(2900)^{--}K^- D^-$. Since the spin parity of $T^a_{c\bar{s}0}$ is established as $I(J^P) = 1(0^+)$, the coupling between $T^a_{c\bar{s}0}$ and KD predominantly occurs through S- and D-wave interactions. Given our focus on studying the production rate of $\bar{T}^a_{c\bar{s}0}(2900)^{--}$ near the threshold region, the contribution from the lowest angular momentum state is most significant. This phenomenon can be attributed to the higher energy requirement for the D-wave production cross section than that of the S-wave production cross section. Thus, in this study, we will employ the effective Lagrangian densities corresponding to the S-wave $\bar{T}^a_{c\bar{s}0}(2900)^{--}K^- D^-$ interaction vertex. It is important to highlight that S-wave effective Lagrangians are always characterized by fewer derivatives. This leads us to express the Lagrangian densities for the S-wave coupling between $\bar{T}^a_{c\bar{s}0}(2900)^{--}$ and $K^- D^-$ as follows [39]:

$$\mathcal{L}_{\bar{T}_{c\bar{s}0}} = g_{\bar{T}_{c\bar{s}0}} \bar{K}^\dagger \vec{\tau} \cdot \bar{T}_{c\bar{s}0} \bar{D}, \tag{4}$$

where the τ is the corresponding Pauli matrix reflecting the isospin of the $\bar{T}^a_{c\bar{s}0}(2900)$. Please note that we have

$$\vec{\tau} \cdot \vec{T}^a_{c\bar{s}0} = \begin{pmatrix} T^a_{c\bar{s}0}(2900)^+ & \sqrt{2} T^a_{c\bar{s}0}(2900)^{++} \\ \sqrt{2} T^a_{c\bar{s}0}(2900)^0 & -T^a_{c\bar{s}0}(2900)^+ \end{pmatrix}, \tag{5}$$

where the state $T^a_{c\bar{s}0}(2900)^+$ has not yet been discovered. It only indicates the signal of $T^a_{c\bar{s}0}(2900)^+$ in the $B^0 \to D^- D^0 K^+$ reaction [41].

In Eq. (4), the coupling constant $g_{\bar{T}_{c\bar{s}0}}$ is determined from the partial decay width of $T^{++}_{c\bar{s}0} \to K^+ D^+$, which is obtained as follows:

$$\Gamma_{T^a_{c\bar{s}0}(2900)^{++} \to K^+ D^+} = \frac{g^2_{T_{c\bar{s}0}}}{4\pi} \frac{|\vec{p}^{\,\text{c.m}}_{D^+}|}{m^2_{T^{++}_{c\bar{s}0}}}, \tag{6}$$

where $\vec{p}^{\,\text{c.m}}_{D^+}$ is the three-vector momentum of the D^+ in the $T^a_{c\bar{s}0}(2900)^{++}$ meson rest frame. Unfortunately, there is no experimental information on the decay widths for $\Gamma(T^a_{c\bar{s}0}(2900)^{++} \to K^+ D^+)$, as this is very difficult to determine. Thus, it is necessary to rely on theoretical predictions, such as those of Refs. [25,28]. Assuming $T^a_{c\bar{s}0}(2900)^{++}$ to be a compact multiquark state, the partial decay width of $T^a_{c\bar{s}0}(2900)^{++} \to K^+ D^+$ is predicted to be $\Gamma(T^{++}_{c\bar{s}0} \to K^+ D^+) = 56.8 \pm 33.4$ MeV [28]. Using the corresponding experimental masses of the relevant particles given in Ref. [42], we obtain $g_{T_{c\bar{s}0}} = 2.836^{+0.739}_{-1.016}$. Note that the partial decay width of $T^a_{c\bar{s}0}(2900)^{++} \to K^+ D^+$ is also evaluated in Ref. [25], adopting the compact multiquark state assignment for $T^a_{c\bar{s}0}(2900)^{++}$, and it is found that the obtained partial decay width falls within the range reported in Ref. [28].

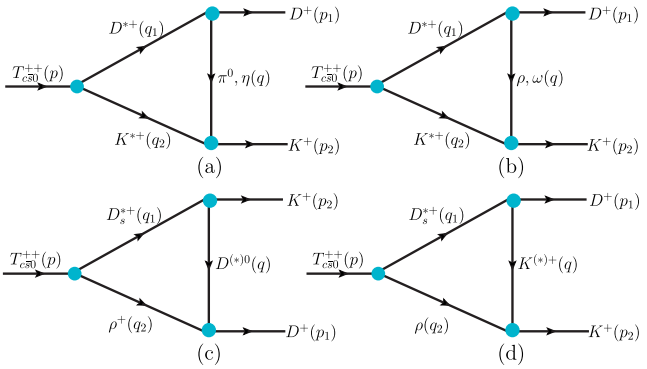

FIG. 2. Feynman diagram contributing to $T^a_{c\bar{s}0}(2900)^{++} \to K^+D^+$. We also show the definition of the kinematics (q, p_1, p_2, q_1, q_2) that we use in the present calculation.

Considering $T^a_{c\bar{s}0}(2900)^{++/0}$ as an S-wave DK-$D_s^*\rho$ molecule [23], we analyze the partial decay width of $T^a_{c\bar{s}0}(2900)^{++}$ into the K^+D^+ final state through hadronic loops with the help of the effective Lagrangians. The loop diagrams are depicted in Fig. 2, and the resulting partial decay widths are provided in Table I. (Additional details can be found in the Appendix.) Utilizing these decay widths, coupling constants are evaluated and collected in Table I.

Since the hadrons are not pointlike particles, it becomes imperative to incorporate form factors when evaluating the scattering amplitudes of the $K^-n \to \bar{T}^a_{c\bar{s}0}(2900)^{--}\Lambda_c^+$ reaction. For the t-channel D^--meson exchange diagram, we adopt a widely used approach found in many previous studies [39,43,44] with the expression

$$\mathcal{F}_{D^-}(q^2_{D^-}, m_{D^-}) = \frac{\Lambda^2_{D^-} - m^2_{D^-}}{\Lambda^2_{D^-} - q^2_{D^-}}, \tag{7}$$

where $q^2_{D^-}$ and m_{D^-} represent the four-momentum and mass of the exchanged D^- meson, respectively. The parameter Λ_{D^-} serves as a hard cutoff, directly linked to the size of the hadron. Empirically, Λ_{D^-} should exceed the m_{D^-} mass by several hundred MeV at least. Therefore, we choose $\Lambda_{D^-} = m_{D^-} + \alpha\Lambda_{\rm QCD}$, following the precedent set by prior works [39,43,44]. The parameter α reflects the nonperturbative property of QCD at the low-energy scale, which will be taken as a parameter and discussed later.

TABLE I. Coupling constants $g_{T_{\bar{c}s0}}$ and the K^+D^+ decay width (in units of MeV) of the $T^a_{c\bar{s}0}(2900)^{++/0}$. The pole positions and effective couplings are evaluated in Ref. [23].

$\sqrt{s}_{\rm pole}$	$\lvert g_{D^*K^*}\rvert$	$\lvert g_{D_s^*\rho}\rvert$	$\Gamma(T^{++}_{c\bar{s}0} \to K^+D^+)$	$g_{T_{\bar{c}s0}}$
2885	5531	5379	48.72–54.59	2.647–2.802
2887	2198	2082	7.37–8.25	1.029–1.089

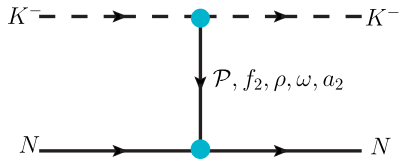

FIG. 3. Feynman diagram for the mechanism of the initial-state interaction of $K^-n \to K^-n$.

In this study, we will examine the impact of the K^-n initial-state interaction on the cross section of $\bar{T}^a_{c\bar{s}0}(2900)^{--}$ production in the $K^-n \to \bar{T}^a_{c\bar{s}0}(2900)^{--}\Lambda_c^+$ reaction. A straightforward approach utilized in Ref. [45] yields a satisfactory representation of the existing experimental data for K^-p and K^-n scattering at high energies. Consequently, we employ this methodology to estimate the initial-state interaction (ISI) in the $K^-n \to K^-n$ reaction at high energies.

The pertinent Feynman diagram depicting the ISI for the $K^-N \to K^-N$ reaction is illustrated in Fig. 3, where exchanges involving the Pomeron and f_2, a_2, ρ, and ω Reggeons (IR) are considered. The total amplitude $\mathcal{T}_{K^-N\to K^-N}$, incorporating Pomeron and Reggeon exchanges, can be expressed as a sum of individual contributions, as indicated by [45]

$$\begin{aligned}\mathcal{T}_{K^-N\to K^-N}(s,t) = {} & \mathcal{A}_{IP}(s,t) + \mathcal{A}_{f_2}(s,t) \pm \mathcal{A}_{a_2}(s,t) \\ & + \mathcal{A}_{\omega}(s,t) \pm \mathcal{A}_{\rho}(s,t),\end{aligned} \tag{8}$$

where $s = (p_1 + p_2)^2$ and $t = (p_1 - q_1)^2$. The $(+)$ and $(-)$ are for the $K^-p \to K^-p$ and $K^-n \to K^-n$ interactions, respectively. For large center-of-mass energies $\sqrt{s}$, the individual contribution to the $\bar{K}N \to \bar{K}N$ amplitude can be parametrized as follows:

$$\mathcal{A}_i(s,t) = \eta_i s \mathcal{C}_i^{KN} \left(\frac{s}{s_0}\right)^{\alpha_i(t)-1} \exp\left(\frac{\mathcal{B}^i_{KN}}{2} t\right), \tag{9}$$

where $i = IP$ represents the Pomeron and f_2, a_2, ω, and ρ are Reggeons. The energy scale is $s_0 = 1\ \text{GeV}^2$. The coupling constants $\mathcal{C}_i^{\bar{K}N}$, the parameters of the Regge linear trajectories $\alpha_i(t) = \alpha_i(0) + \alpha_i' t$, the signature factors η_i, and the $\mathcal{B}^i_{\bar{K}N}$ utilized in Ref. [45] offer a suitable description of the experimental data. The parameters determined in Ref. [45] are outlined in Table II.

Using the effective Lagrangians mentioned above and taking the ISI of the K^-p system into account, the full amplitude of the $K^-n \to \bar{T}^a_{c\bar{s}0}(2900)^{--}\Lambda_c^+$ reaction can be derived as

$$\mathcal{M}^{\rm full} = \mathcal{M}^{\rm Born} + \mathcal{M}^{K^-n-{\rm ISI}}, \tag{10}$$

where the Born amplitude is written as

TABLE II. Parameters of Pomeron and Reggeon exchanges determined from elastic and total cross sections in Ref. [45].

i	η_i	$\alpha_i(t)$	$\mathcal{C}_i^{KN}$(mb)	$\mathcal{B}_i^{KN}$ (GeV^{-2})
IP	i	$1.081 + (0.25\ \mathrm{GeV}^{-2})t$	11.82	5.5
f_2	$-0.861 + i$	$0.548 + (0.93\ \mathrm{GeV}^{-2})t$	15.67	4.0
ρ	$-1.162 - i$	$0.548 + (0.93\ \mathrm{GeV}^{-2})t$	2.05	4.0
ω	$-1.162 - i$	$0.548 + (0.93\ \mathrm{GeV}^{-2})t$	7.055	4.0
a_2	$-0.861 + i$	$0.548 + (0.93\ \mathrm{GeV}^{-2})t$	1.585	4.0

$$\mathcal{M}^{\mathrm{Born}} = if_I g_{\bar{T}_{c\bar{s}0}} g_{\Lambda_c ND} \bar{u}(q_2, s_{\Lambda_c^+}) \gamma_5 u(p_2, s_p) \times \frac{i}{(q_1 - p_1)^2 - m_{D^-}^2} \mathcal{F}_{D^-}[(q_1 - p_1)^2_{D^-}, m_{D^-}], \quad (11)$$

and the corrections to the Born amplitude due to $K^- n$ interactions were taken into account in Refs. [45,46] as

$$\mathcal{M}^{K^- n\text{–ISI}} = \frac{i}{16\pi^2 s} \int d^2\vec{k}_t \mathcal{T}_{K^- n \to K^- n}(s, k_t^2) \mathcal{M}^{\mathrm{Born}}, \quad (12)$$

where k_t is the momentum transfer in the $K^- n \to K^- n$ reaction, $\bar{u}(q_2, s_{\Lambda_c^+})$ and $u(p_2, s_p)$ are the Dirac spinors, and $s_{\Lambda_c^+}(q_2)$ and $s_p(p2)$ are the spins (the four-momenta) of the outgoing Λ_c^+ and the initial proton, respectively.

With the scattering amplitudes of the $K^- n \to \bar{T}^a_{c\bar{s}0}(2900)^{--}\Lambda_c^+$ reaction obtained in the previous section, the differential cross section in the center of mass (c.m.) frame for the process $K^- n \to \bar{T}^a_{c\bar{s}0}(2900)^{--}\Lambda_c^+$ can be calculated as [42]

$$\frac{d\sigma}{d\cos\theta} = \frac{m_N m_{\Lambda_c^+}}{4\pi s} \frac{|\vec{q}_{1\mathrm{c.m.}}|}{|\vec{p}_{1\mathrm{c.m.}}|} \left(\frac{1}{2} \sum_{s_n, s_{\Lambda_c^+}} |\mathcal{M}|^2 \right), \quad (13)$$

where the θ is the scattering angle of the outgoing $\bar{T}^a_{c\bar{s}0}$ meson relative to the beam direction, while $\vec{p}^{\,1\mathrm{c.m.}}$ and $\vec{q}^{\,1\mathrm{c.m.}}$ are the K^-- and $\bar{T}^a_{c\bar{s}0}$-meson three-momenta in the center-of-mass frame, respectively, which are

$$|\vec{p}_{1\mathrm{c.m.}}| = \frac{\lambda^{1/2}(s, m_{K^-}, m_n)}{2\sqrt{s}}, \quad |\vec{q}_{1\mathrm{c.m.}}| = \frac{\lambda^{1/2}(s, m_{T^a_{c\bar{s}0}}, m_{\Lambda_c^+})}{2\sqrt{s}}. \quad (14)$$

Here, $\lambda(x, y, z) = (x - y - z)^2 - 4yz$ is the Källen function.

III. RESULTS AND DISCUSSIONS

With the formalism and ingredients given above, the cross section as a function of the beam momentum P_{K^-} for the $K^- n \to \bar{T}^a_{c\bar{s}0}(2900)^{--}\Lambda_c^+$ reaction can be easily obtained. Before presenting the results, it is important to discuss the parameter α that relates to the form factor. This is because the value of the cross section is highly sensitive to the model parameter α. However, determining the value of α from first principles is currently not feasible. Instead, it can be better determined from the experimental data. Indeed, it has been established that the free parameter values of $\alpha = 1.5$ or 1.7 were fixed by fitting the experimental data of the processes $e^+e^- \to D\bar{D}$ [47] and $e^+e^- \to \gamma\mathrm{ISR}D\bar{D}$ [48]. The procedure for this fitting is outlined in Ref. [49]. For this study, we adopt the values $\alpha = 1.5$ or 1.7, as they have been determined from the experimental data of Refs. [47,48] using the same D form factors employed in our current work.

With the obtained α value, the cross section for the $K^- n \to \bar{T}^a_{c\bar{s}0}(2900)^{--}\Lambda_c^+$ reaction is evaluated by treating $T^a_{c\bar{s}0}$ as a compact multiquark state. The theoretical results obtained with a cutoff $\alpha = 1.5$ or 1.7 for the beam energy from near threshold up to 27.5 GeV are shown in Fig. 4. We can find that the cross section exhibits a sharp increase near the threshold of $\bar{T}^a_{c\bar{s}0}(2900)^{--}\Lambda_c^+$, an effect attributed to the opening of phase space at that energy. Following this, the cross section continues to increase, albeit at a comparatively slower rate than the threshold region. However, a modest decline in the cross section is observed as the beam energy P_{K^-} is varied from 23.1 to 27.5 GeV. For deeper insight, we illustrate the obtained total cross section behavior, ranging from approximately 0.268 nb to 0.254 nb for $\alpha = 1.5$, with varying beam momentum from 23.25 GeV to 26.80 GeV. Within the same energy range, but adopting $\alpha = 1.7$, the cross section spans from 0.320 nb to 0.338 nb. These outcomes suggest that the value of the cross section is not very sensitive to the model parameter α when varying the cutoff parameter α from 1.5 to 1.7.

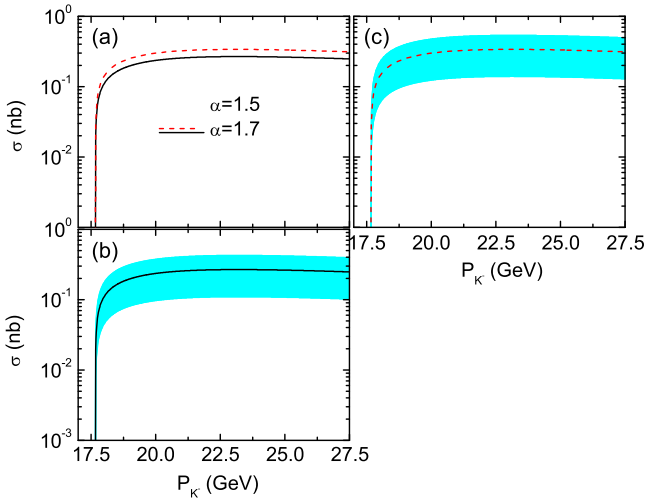

FIG. 4. The cross section for the $K^- n \to \bar{T}^a_{c\bar{s}0}(2900)^{--}\Lambda_c^+$ reaction as a function of the beam momentum P_{K^-}, assuming $\bar{T}^a_{c\bar{s}0}$ as a compact tetraquark state. The central values displayed in panel (a) correspond to the coupling constant $g_{T_{c\bar{s}0}} = 2.836$, and the cyan bands in (b) and (c) denote the cross sections for different $\Gamma(T^{++}_{c\bar{s}0} \to K^+ D^+)$ values [28].

In addition to showing the central values of the cross sections corresponding to $g_{T_{c\bar{s}0}} = 2.836$ in Fig. 4(a), we also present the variation of the cross sections for different $g_{T_{c\bar{s}0}}$ values, which are determined based on the theoretically predicted partial decay width of $T^{++}_{c\bar{s}0} \to K^+D^+$ [28]. We depict the results for the cutoffs $\alpha = 1.5$ and $\alpha = 1.7$ in Figs. 4(b) and 4(c), respectively. Remarkably, significant variations in the cross sections are observed. For $\alpha = 1.5$, the obtained cross section ranges from 0.104 nb to 0.402 nb, and for $\alpha = 1.7$, it ranges from 0.132 nb to 0.506 nb, both at an example energy of approximately $P_{K^-} = 26.80$ GeV. This suggests that the cross section for the maximum value is about 4 times larger than that of the minimum value. This discrepancy can be attributed to the fact that the ratio of the coupling constant for the maximum value to that of the minimum value is around 2.0, and the cross section is proportional to the square of the coupling constant.

We now shift our focus to the cross section of the $K^-n \to \bar{T}^a_{c\bar{s}0}(2900)^{--}\Lambda_c^+$ reaction, considering $T^a_{c\bar{s}0}(2900)$ as a K^*D^*-$D_s^*\rho$ molecule. The cross section, varying with the beam energy P_{K^-} from just above the threshold up to 27.5 GeV, is depicted in Fig. 5. We clearly observe that the line shapes of the cross sections mirror those obtained by considering $T^a_{c\bar{s}0}(2900)$ as a compact multiquark state. That means that the cross section also increases sharply near the threshold, followed by a gradual and sustained increase at higher energies, concluding with a gradual decrease.

The results in Fig. 5 also tell us that the $\bar{T}^a_{c\bar{s}0}(2900)^{--}$ production cross section for the cutoff $\alpha = 1.5$ is slightly smaller than that for the cutoff $\alpha = 1.7$. The variation of the cross sections for different $\Gamma(T^{++}_{c\bar{s}0} \to K^+D^+)$ values is very small. To see how much the cross section depends on the $\Gamma(T^{++}_{c\bar{s}0} \to K^+D^+)$ decay widths and the cutoff α, we take the cross section at a beam momentum of about $P_{K^-} = 25.0$ GeV and the mass of the bound state $m = 2885$ MeV as an example. The so-obtained cross section

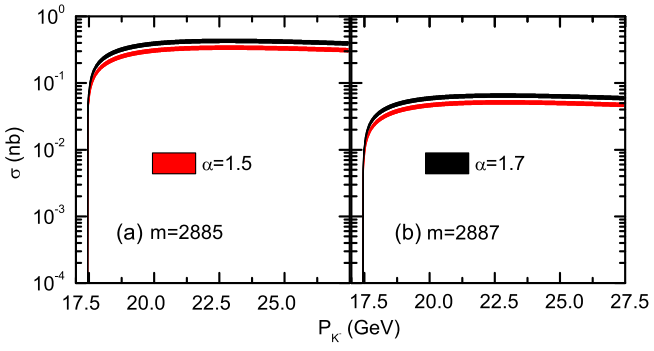

FIG. 5. The cross section for the $K^-n \to \bar{T}^a_{c\bar{s}0}(2900)^{--}\Lambda_c^+$ reaction as a function of the beam momentum P_{K^-}, assuming $\bar{T}^a_{c\bar{s}0}$ as a K^*D^*-$D_s^*\rho$ molecule. The color bands denote the cross sections for different $\Gamma(T^{++}_{c\bar{s}0} \to K^+D^+)$ values, and m is the mass of the bound states $T^a_{c\bar{s}0}(2900)$ obtained in Ref. [23].

ranges from 0.302 nb to 0.350 nb for $\alpha = 1.5$, and from 0.394 nb to 0.442 nb for $\alpha = 1.7$. We also find that if the $\bar{T}^a_{c\bar{s}0}(2900)$ is produced as a K^*D^*-$D_s^*\rho$ molecule with mass $m = 2885$ MeV, the cross section is significantly larger than the results obtained by assuming $\bar{T}^a_{c\bar{s}0}(2900)$ as a KD-$D_s^*\rho$ molecule with mass $m = 2887$ MeV, by about 6–8 times. In other words, the cross section heavily depends on the masses of the bound states. The primary cause of the substantial difference in the production cross section, despite the small 2 MeV difference in the bound-state mass, lies in the significant disparity in their interactions with the molecular component DK [23]. We find that the coupling constant for the bound state with $m = 2885$ is 2.52 times larger than that of the bound state with $m = 2887$ (see the second column of Table I). This leads to the coupling constants $g_{T_{c\bar{s}0}}$ for the bound state with $m = 2885$ being 2.6–2.8 times larger than that of the bound state with $m = 2887$, resulting in a nearly 1-order-of-magnitude change in the cross section.

By comparing the cross sections depicted in Figs. 4 and 5, we observe that if $\bar{T}^a_{c\bar{s}0}(2900)^{--}$ is a compact tetraquark state, its production cross sections match the results predicted by considering $\bar{T}^a_{c\bar{s}0}(2900)^{--}$ as a K^*D^*-$D_s^*\rho$ molecule with a mass of $m = 2885$ MeV. Specifically, the cross sections for these two assignments can reach 0.538 nb (for the compact tetraquark state) and 0.454 nb (for the K^*D^*-$D_s^*\rho$ molecule). These results suggest that if $\bar{T}^a_{c\bar{s}0}(2900)$ is a K^*D^*-$D_s^*\rho$ molecule with a mass of $m = 2887$ MeV, distinguishing its K^*D^*-$D_s^*\rho$ molecular nature from the compact tetraquark state is challenging through the $K^-n \to \bar{T}^a_{c\bar{s}0}(2900)^{--}\Lambda_c^+$ reaction. However, when considering a smaller cross-section obtained from the assumption that $\bar{T}^a_{c\bar{s}0}(2900)^{--}$ is a K^*D^*-$D_s^*\rho$ molecule with a mass of $m = 2887$ MeV, the cross section is limited to 0.068 nb. This discrepancy magnifies the difference between the results of the two scenarios by a factor of about 8.0. This indicates that if the mass of the K^*D^*-$D_s^*\rho$ molecule is $m = 2887$ MeV, a clear conclusion about the nature of $\bar{T}^a_{c\bar{s}0}(2900)$ can be easily obtained by comparing the obtained cross section with future experimental data.

However, a clearer comparison can be drawn from the production of $\bar{T}^a_{c\bar{s}0}(2900)$ in the $K^-n \to \bar{T}^a_{c\bar{s}0}(2900)^{--}\Lambda_c^+ \to \pi^-D_s^-\Lambda_c^+$ reaction, and the results of this comparison are shown in Fig. 6. We find that the cross section for the molecule assignment of $\bar{T}^a_{c\bar{s}0}(2900)$ can reach up to 3.66×10^{-3} nb. This value is significantly smaller than that of 0.244 nb at the same beam energy, and the larger cross section is derived from the compact tetraquark state assignment of $\bar{T}^a_{c\bar{s}0}(2900)$. The significant difference between the results in these two pictures arises from considering $T^a_{c\bar{s}0}(2900)$ in two different ways. If it is seen as a compact tetraquark state, the calculated partial decay width of $T^a_{c\bar{s}0}(2900)^{++} \to \pi^+D_s^+$ is 48.5 ± 30.0 MeV [28] (we use 78.5 MeV). This contrasts sharply with the range of 0.132–

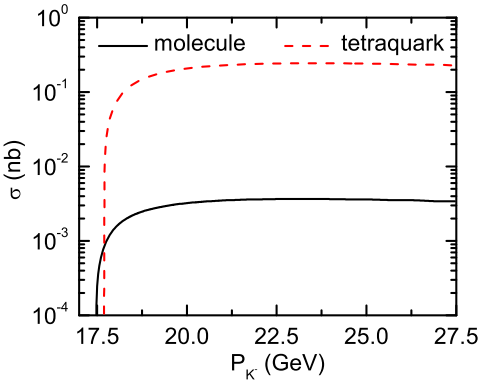

FIG. 6. The cross sections for the $K^- n \to \bar{T}^a_{c\bar{s}0}(2900)^{--}\Lambda_c^+ \to \pi^- D_s^- \Lambda_c^+$ reaction as a function of the beam momentum P_{K^-}, assuming $\bar{T}^a_{c\bar{s}0}$ to be a K^*D^*-$D_s^*\rho$ molecule (black solid line) or a compact tetraquark state (red dashed line). Here, we display results associated with $\alpha = 1.7$, the bound-state mass $m = 2885$ MeV, and the maximum value of the coupling constants $g_{T^a_{c\bar{s}0}}$.

1.167 MeV (we use 1.167 MeV) obtained by treating $T^a_{c\bar{s}0}(2900)$ as a K^*D^*-$D_s^*\rho$ molecule with a mass of $m = 2885$ MeV. Importantly, the partial decay width of $T^a_{c\bar{s}0}(2900)^{++} \to \pi^+ D_s^+$ from the $D_s^*\rho$-channel contribution is prohibited, and the necessary amplitudes required for the $T^a_{c\bar{s}0}(2900)^{++} \to \pi^+ D_s^+$ reaction in our work are available in Ref. [21]. Note that the cross section for the $K^- n \to \pi^- D_s^- \Lambda_c^+$ reaction are computed from the following differential cross section [50]:

$$\frac{d\sigma_{K^- n \to \pi^- D_s^- \Lambda_c^+}}{d\mathcal{M}_{\pi^- D_s^-}} \approx \frac{2 m_{\bar{T}^a_{c\bar{s}0}} \mathcal{M}_{\pi^- D_s^-}}{\pi} \times \frac{\sigma_{K^- n \to \bar{T}^a_{c\bar{s}0}(2900)^{--}\Lambda_c^+} \Gamma_{\bar{T}^a_{c\bar{s}0}(2900)^{--} \to \pi^- D_s^-}}{(\mathcal{M}^2_{\pi^- D_s^-} - m^2_{\bar{T}^a_{c\bar{s}0}})^2 + m^2_{\bar{T}^a_{c\bar{s}0}} \Gamma^2_{\bar{T}^a_{c\bar{s}0}}}, \tag{15}$$

where $m_{\bar{T}^a_{c\bar{s}0}}$ and $\Gamma_{\bar{T}^a_{c\bar{s}0}}$ are the mass and width of $\bar{T}^a_{c\bar{s}0}$, respectively. $\mathcal{M}_{\pi^- D_s^-}$ is in the range of $(m_{\pi^-} + m_{D_s^-})$–$(\sqrt{s} - m_{\Lambda_c^+})$.

Considering isospin symmetry, the decay width of K^+D^0 for the unreported $T^a_{c\bar{s}0}(2900)^+$ state is expected to be half of the partial decay width of $T^{++}_{c\bar{s}0} \to K^+D^+$ [as seen in Eq. (5)]. If we regard $T^a_{c\bar{s}0}(2900)^+$ as a K^*D^*-$D_s^*\rho$ molecule, the predicted partial decay widths for the bound state with the masses $m = 2885$ MeV and $m = 2887$ MeV are $\Gamma(T^+_{c\bar{s}0} \to K^+D^0) = 24.36$–$27.30$ MeV and $\Gamma(T^+_{c\bar{s}0} \to K^+D^0) = 2.69$–$4.13$ MeV, respectively. Furthermore, the decay width $\Gamma(T^+_{c\bar{s}0} \to K^+D^0)$ is estimated to be within the range of 11.7–45.1 MeV when considering $T^+_{c\bar{s}0}$ as a compact tetraquark state. These predictions open up an opportunity to search for $\bar{T}^a_{c\bar{s}0}(2900)^-$ [$\bar{T}^a_{c\bar{s}0}(2900)^-$ is the antiparticle of $T^a_{c\bar{s}0}(2900)^+$] in the $K^- p \to \bar{T}^a_{c\bar{s}0}(2900)^-\Lambda_c^+$ reaction. The cross section for the $K^- p \to \bar{T}^a_{c\bar{s}0}(2900)^-\Lambda_c^+$ reaction, with a cutoff $\alpha = 1.7$ and a beam momentum P_{K^-} ranging from the near threshold to 27.5 GeV, is presented in Fig. 7. Our findings reveal that the maximum value of the cross section for $\bar{T}^a_{c\bar{s}0}(2900)^-$ production in the $K^- p \to \bar{T}^a_{c\bar{s}0}(2900)^-\Lambda_c^+$ reaction is approximately 0.228 nb, which is bigger than 0.150 nb, the maximum value reached by assigning $\bar{T}^a_{c\bar{s}0}(2900)^-$ as a compact tetraquark state.

It is worth noting that the contributions to the $K^- p \to \bar{T}^a_{c\bar{s}0}(2900)^-\Lambda_c^+$ reaction are mediated by the exchange of D mesons in the t channel, which is identical to the production process of its isospin partner $\bar{T}^a_{c\bar{s}0}(2900)^{--}$. The only difference is the influence of $\bar{K}N$ ISI on their product cross sections. To show the effect from the $\bar{K}N$ ISI, we compare the cross sections obtained with and without ISI for the cutoff $\alpha = 1.7$ and $g_{T_{c\bar{s}0}} = 2.836$ in Fig. 8, for the $K^- n \to \bar{T}^a_{c\bar{s}0}(2900)^{--}\Lambda_c^+$ [Fig. 8(a)] and $K^- p \to \bar{T}^a_{c\bar{s}0}(2900)^-\Lambda_c^+$ [Fig. 8(b)] reactions. In Fig. 8, the solid black line is the pure Born amplitude contribution, while the dashed red line shows the full results. We can find that the presence of the $\bar{K}N$ ISI leads to a reduction in the cross section of the $K^- p \to \bar{T}^a_{c\bar{s}0}(2900)^-\Lambda_c^+$ and $K^- p \to \bar{T}^a_{c\bar{s}0}(2900)^-\Lambda_c^+$ reactions by approximately 20%. This suggests that the $\bar{K}N$ ISIs have a significant impact on the search for $\bar{T}^a_{c\bar{s}0}(2900)$ in the $K^- N \to \bar{T}^a_{c\bar{s}0}(2900)^{-/--}\Lambda_c^+$ reactions. Similar conclusions regarding the reduction in the cross section could be drawn if one were to consider $\bar{T}^a_{c\bar{s}0}(2900)$ as a KD-$D_s^*\rho$ molecule, and we here do not discuss it in detail.

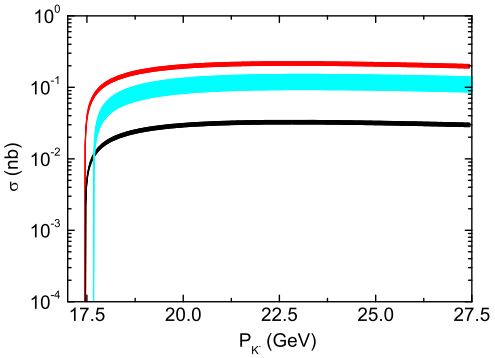

FIG. 7. The cross section for the $K^- p \to \bar{T}^a_{c\bar{s}0}(2900)^-\Lambda_c^+$ reaction as a function of the beam momentum P_{K^-}, assuming $\bar{T}^a_{c\bar{s}0}$ to be a K^*D^*-$D_s^*\rho$ molecule (red and black bands) or a compact tetraquark (cyan bands). The color bands denote the cross sections for different $\Gamma(T^+_{c\bar{s}0} \to K^+D^0)$ values. The red and black bands correspond to the bound-state masses $m = 2885$ MeV and $M = 2887$ MeV, respectively, obtained in Ref. [23]. The cyan band is the cross section for the mass of the bound state $m = 2921$ MeV [18].

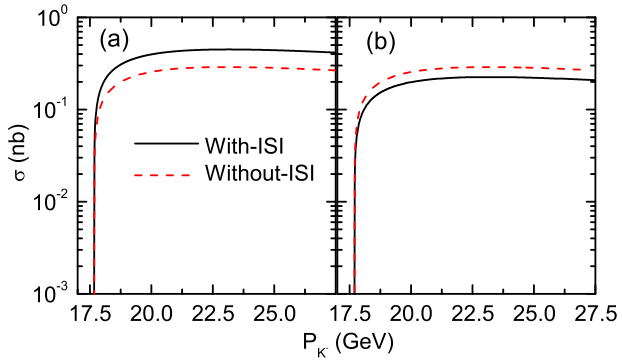

FIG. 8. The cross sections for the $K^- p \to \bar{T}^a_{c\bar{s}0}(2900)^- \Lambda_c^+$ and $K^- p \to \bar{T}^a_{c\bar{s}0}(2900)^- \Lambda_c^+$ reactions as a function of the beam momentum P_{K^-}, assuming $\bar{T}^a_{c\bar{s}0}$ to be a compact tetraquark state. The solid black lines and dashed red lines represent the cross sections obtained with and without ISI, respectively.

IV. SUMMARY

Theoretical investigations into the production processes will be helpful to distinguish which inner structure of $T^a_{c\bar{s}0}(2900)$ is possible. This is because the different production mechanisms of $T^a_{c\bar{s}0}(2900)$ rely on its structure assignments. In this work, we examine the recently observed $\bar{T}^a_{c\bar{s}0}(2900)$ production in the $K^- n \to \bar{T}^a_{c\bar{s}0}(2900)^{--} \Lambda_c^+$ and $K^- n \to \bar{T}^a_{c\bar{s}0}(2900)^{--} \Lambda_c^+ \to \pi^- D_s^- \Lambda_c^+$ reactions by considering $T^a_{c\bar{s}0}$ as a molecular state and as a compact multiquark state, respectively. The $T^a_{c\bar{s}0}(2900)$ can be produced though the exchange of D mesons in the t channel.

Using the coupling constants of the $\bar{T}^a_{c\bar{s}0}(2900)$ to the KD channel obtained from the molecule or compact tetraquark picture of $\bar{T}^a_{c\bar{s}0}(2900)$, we compute the cross sections for the $K^- n \to \bar{T}^a_{c\bar{s}0}(2900)^{--} \Lambda_c^+$ and $K^- n \to \bar{T}^a_{c\bar{s}0}(2900)^{--} \Lambda_c^+ \to \pi^- D_s^- \Lambda_c^+$ reactions. The numerical results reveal that whether $\bar{T}^a_{c\bar{s}0}(2900)$ is categorized as a molecule or a compact tetraquark state, the cross sections for the $K^- n \to \bar{T}^a_{c\bar{s}0}(2900)^{--} \Lambda_c^+$ reaction exhibit similar magnitudes, spanning roughly from 0.12 nb to 0.6 nb. Nevertheless, a more distinct comparison can be drawn by computing the cross section of the $K^- n \to \bar{T}^a_{c\bar{s}0}(2900)^{--} \Lambda^+ c \to \pi^- D_s^- \Lambda_c^+$ process. The results indicate that, assuming the molecule assignment for $\bar{T}^a_{c\bar{s}0}(2900)$, the cross section for the $K^- n \to \bar{T}^a_{c\bar{s}0}(2900)^{--} \Lambda^+ c \to \pi^- D_s^- \Lambda_c^+$ reaction could peak at 3.66×10^{-3} nb, notably smaller than the 0.244 nb obtained by presuming $\bar{T}^a_{c\bar{s}0}(2900)$ to be a compact tetraquark state. These findings are poised for future experimental measurement and can serve as tests to discern the nature of $\bar{T}^a_{c\bar{s}0}(2900)$. Lastly, we suggest a quest for the unreported charged tetraquark $T^a_{c\bar{s}0}(2900)^+$ in the $K^- p \to \bar{T}^a_{c\bar{s}0}(2900)^- \Lambda_c^+$ reaction, given the fact that its production cross section can reach up to 0.228 nb.

A rough estimation finds that the production cross section of the $\bar{T}^a_{c\bar{s}0}(2900)$ through high-energy proton-proton collisions is approximately 17 fb (see Fig. 3 in Ref. [18]). This value is about 10^4 times smaller than our calculated results. This difference is why we propose to search for $\bar{T}^a_{c\bar{s}0}(2900)$ in the reactions $K^- p \to \bar{T}^a_{c\bar{s}0}(2900)^- \Lambda_c^+$ and $K^- n \to \bar{T}^a_{c\bar{s}0}(2900)^{--} \Lambda_c^+ \to \pi^- D_s^- \Lambda_c^+$. Furthermore, kaon beams with momenta ranging from 50 to 280 GeV/c and an rms below 5% are available from the M2 beamline at AMBER [36]. AMBER is a new fixed-target experiment at CERN that began its data-taking in 2023, providing an excellent platform for the search for $\bar{T}^a_{c\bar{s}0}(2900)$.

ACKNOWLEDGMENTS

This work was supported by the National Natural Science Foundation of China under Grant No. 12005177.

APPENDIX: PARTIAL DECAY WIDTHS $T^a_{c\bar{s}0}(2900)^{++} \to K^+ D^+$

In this appendix, we show how to compute the partial decay width of the $T^a_{c\bar{s}0}(2900)^{++} \to K^+ D^+$ reaction. The corresponding Feynman diagrams are shown in Fig. 2. To compute the diagrams, we require the effective Lagrangian densities for the relevant interaction vertices. Since $T^a_{c\bar{s}0}(2900)^{++}$ resonance can be identified as an S-wave $D^* K^*$-ρD_s^* molecule [23], the Lagrangian densities for the $T^a_{c\bar{s}0}(2900)^{++} D^* K^*$ and $T^a_{c\bar{s}0}(2900)^{++} \rho D_s^*$ vertices can be written down as [41]

$$\mathcal{L}_{T^a_{c\bar{s}0} K^* D^*} = g_{T^a_{c\bar{s}0} K^* D^*} D^{*\mu} \vec{\tau} \cdot \vec{T}^a_{c\bar{s}0} K^*_\mu, \tag{A1}$$

$$\mathcal{L}_{T^a_{c\bar{s}0} \rho D_s^*} = g_{T^a_{c\bar{s}0} \rho D_s^*} D_s^{*\mu} \vec{\rho}_\mu \cdot \vec{T}^a_{c\bar{s}0}, \tag{A2}$$

where the coupling constants $g_{T^a_{c\bar{s}0} K^* D^*} = 2.198$–$5.531$ GeV and $g_{T^a_{c\bar{s}0} \rho D_s^*} = 2.082$–$5.379$ GeV, which correspond to the physical sheet [23].

Considering the heavy quark limit and chiral symmetry, the relevant phenomenological Lagrangians for the $\mathcal{D}^* \mathcal{D} \mathcal{P}$ and $\mathcal{D}^* \mathcal{D} \mathcal{V}$ vertices are [21,51,52]

$$\mathcal{L}_{\mathcal{D}^* \mathcal{D} \mathcal{P}} = ig \langle \mathcal{D}^*_\mu u^\mu \mathcal{D}^\dagger - \mathcal{D} u^\mu \mathcal{D}^{*\dagger}_\mu \rangle, \tag{A3}$$

$$\mathcal{L}_{\mathcal{D}^* \mathcal{D} \mathcal{V}} = -2 f_{D^* D \mathcal{V}} \epsilon_{\mu\nu\alpha\beta} (\partial^\mu \mathcal{V}^\nu)^i_j \times (\mathcal{D}_i \overleftrightarrow{\partial}_\alpha \mathcal{D}^{*\beta j\dagger} - \mathcal{D}^{*\beta}_i \overleftrightarrow{\partial}_\alpha \mathcal{D}^{j\dagger}), \tag{A4}$$

where the $\langle \ldots \rangle$ denotes a trace in the SU(3) flavor space and $\epsilon^{0123} = 1$. $\mathcal{P}$ and $\mathcal{V}^\mu$ are the SU(3) pseudoscalar meson and vector meson matrices, respectively:

$$\mathcal{P} = \begin{pmatrix} \frac{1}{\sqrt{2}}\pi^0 + \frac{1}{\sqrt{6}}\eta & \pi^+ & K^+ \\ \pi^- & -\frac{1}{\sqrt{2}}\pi^0 + \frac{1}{\sqrt{6}}\eta & K^0 \\ K^- & \bar{K}^0 & -\frac{2}{\sqrt{6}}\eta \end{pmatrix}, \tag{A5}$$

$$\mathcal{V}_\mu = \begin{pmatrix} \frac{1}{\sqrt{2}}(\rho^0+\omega) & \rho^+ & K^{*+} \\ \rho^- & \frac{1}{\sqrt{2}}(-\rho^0+\omega) & K^{*0} \\ K^{*-} & \bar{K}^{*0} & \phi \end{pmatrix}_\mu, \quad \text{(A6)}$$

and $\mathcal{D}^{(*)} = (D^{(*)0}, D^{(*)+}, D_s^{*(+)})$. u^μ is the axial vector combination of the pseudoscalar meson fields, and at the lowest order, $u^2 = -\sqrt{2}\partial^\mu \mathcal{P}/f_0$, with $f_0 = 92.4$ MeV. The coupling constants $f_{D^*D\mathcal{V}} = \lambda m_\rho/(\sqrt{2}f_\pi)$, with $\lambda = 0.56\ \text{GeV}^{-1}$, $f_\pi = 132$ MeV [51], and m_ρ is the mass of the ρ meson. The coupling constant $g = 1.097$ is determined from the strong decay width $\Gamma(D^{*+} \to D^0\pi^+) = 56.46 \pm 1.22$ keV, together with the branching ratio $\text{BR}(D^{*+} \to D^0\pi^+) = (67.7 \pm 0.5)\%$.

For the ρDD and $KD^*D_s^*$ vertices, the following effective Lagrangians are needed [53–55]:

$$\mathcal{L}_{DD\rho} = ig_{DD\rho}(D^\dagger \vec{\tau}\cdot\vec{\rho}^\mu \partial_\mu \bar{D} - \partial_\mu D^\dagger \vec{\tau}\cdot\vec{\rho}^\mu \bar{D}), \quad \text{(A7)}$$

$$\mathcal{L}_{KD_s^*D^*} = -g_{KD_s^*D^*}\epsilon^{\mu\nu\alpha\beta}(\partial_\mu \bar{D}^{*\dagger}_\nu \partial_\alpha D^*_{s\beta}\bar{K} + \partial_\mu D^{*\dagger}_\nu \partial_\alpha \bar{D}^*_{s\beta} K), \quad \text{(A8)}$$

where the coupling constant $g_{DD\rho} = 2.52$ [54] is derived from the D-meson electric form factor in the standard framework of the vector meson dominance model. $g_{KD_s^*D^*} = 7.0\ \text{GeV}^{-1}$ was computed from the SU(4) relations [55]. The charm- and K-meson isodoublets are defined as

$$\bar{D}^{(*)\dagger} = (\,\bar{D}^{(*)0} \quad D^{(*)-}\,), \qquad D^{(*)} = \begin{pmatrix} D^{(*)0} \\ D^{(*)+} \end{pmatrix}, \quad \text{(A9)}$$

$$\bar{K}^{(*)\dagger} = (\,K^{(*)-} \quad \bar{K}^{(*)0}\,), \qquad K^{(*)} = \begin{pmatrix} K^{(*)+} \\ K^{(*)0} \end{pmatrix}. \quad \text{(A10)}$$

In addition to the vertices described above, we also need the following effective Lagrangians [21]:

$$\mathcal{L}_{\mathcal{PPV}} = -ig_h\langle[\mathcal{P}, \partial^\mu \mathcal{P}]\mathcal{V}_\mu\rangle, \quad \text{(A11)}$$

$$\mathcal{L}_{K^*K\mathcal{V}'} = -g_{K^*K\mathcal{V}'}\epsilon^{\mu\nu\alpha\beta}\partial_\alpha \bar{K}^*_\beta \partial_\mu \mathcal{V}'_\nu K + \text{H.c.}, \quad \text{(A12)}$$

where $\mathcal{V}'$ signifies meson matrices:

$$\mathcal{V}'_\mu = \begin{pmatrix} \frac{1}{\sqrt{2}}(\rho^0+\omega) & \rho^+ \\ \rho^- & \frac{1}{\sqrt{2}}(-\rho^0+\omega) \end{pmatrix}_\mu. \quad \text{(A13)}$$

The coupling constant $g_{K^*K\mathcal{V}'} = 3g_h^2/(64\pi^2 f_\pi)$ with g_h is determined via the measured width of $K^* \to \pi K$. With the help of Eq. (A11), the two-body decay width $K^* \to K\pi$ is related to g_h as

$$\Gamma(K^{*+} \to K^0\pi^+) = \frac{g^2}{24\pi m_{K^{*+}}^2}\mathcal{P}^3_{\pi K^*} = \frac{2}{3}\Gamma_{K^{*+}}, \quad \text{(A14)}$$

where $\mathcal{P}_{\pi K^*}$ is the three-momentum of the π in the rest frame of the K^*. Using the experimental strong decay width ($\Gamma_{K^{*+}} = 50.3 \pm 0.8$ MeV) and the masses of the particles shown in Ref. [42], we obtain $g_h = 9.11$.

Putting all the pieces together, we obtain the following strong decay amplitudes:

$$\mathcal{M}_a^{\pi^0} = -i\frac{gg_h g_{T^a_{c\bar{s}0}}}{f_0}\int \frac{d^4q}{(2\pi)^4} q_\mu \frac{-g^{\mu\nu} + q_1^\mu q_1^\nu/m_{D^{*+}}^2}{q_1^2 - m_{D^{*+}}^2} \times \frac{-g^{\nu\sigma} + q_2^\nu q_2^\sigma/m_{K^{*+}}^2}{q_2^2 - m_{K^{*+}}^2}(q_\sigma + p_{2\sigma})\frac{1}{q^2 - m_{\pi^0}^2}, \quad \text{(A15)}$$

$$\mathcal{M}_a^{\eta} = i\frac{gg_h g_{T^a_{c\bar{s}0}}}{3f_0}\int \frac{d^4q}{(2\pi)^4} q_\mu \frac{-g^{\mu\nu} + q_1^\mu q_1^\nu/m_{D^{*+}}^2}{q_1^2 - m_{D^{*+}}^2} \times \frac{-g^{\nu\sigma} + q_2^\nu q_2^\sigma/m_{K^{*+}}^2}{q_2^2 - m_{K^{*+}}^2}(q_\sigma + p_{2\sigma})\frac{1}{q^2 - m_{\eta}^2}, \quad \text{(A16)}$$

$$\mathcal{M}_b^{\rho^0} = -i\sqrt{2}f_{D^*D\rho}g_{T^a_{c\bar{s}0}}g_{K^*K\rho}\int \frac{d^4q}{(2\pi)^4}\epsilon_{\mu\nu\alpha\beta}q^\mu \times (p_1^\alpha + q_1^\alpha)\frac{-g^{\beta\sigma} + q_1^\beta q_1^\sigma/m_{D^{*+}}^2}{q_1^2 - m_{D^{*+}}^2}\frac{-g^{\sigma\eta} + q_2^\sigma q_2^\eta/m_{K^{*+}}^2}{q_2^2 - m_{K^{*+}}^2} \times \epsilon_{\tau\lambda\kappa\eta}q_2^\kappa q^\tau \frac{-g^{\lambda\nu} + q^\lambda q^\nu/m_{\rho^0}^2}{q^2 - m_{\rho^0}^2}, \quad \text{(A17)}$$

$$\mathcal{M}_b^{\omega} = i\sqrt{2}f_{D^*D\omega}g_{T^a_{c\bar{s}0}}g_{K^*K\omega}\int \frac{d^4q}{(2\pi)^4}\epsilon_{\mu\nu\alpha\beta}q^\mu \times (p_1^\alpha + q_1^\alpha)\frac{-g^{\beta\sigma} + q_1^\beta q_1^\sigma/m_{D^{*+}}^2}{q_1^2 - m_{D^{*+}}^2}\frac{-g^{\sigma\eta} + q_2^\sigma q_2^\eta/m_{K^{*+}}^2}{q_2^2 - m_{K^{*+}}^2} \times \epsilon_{\tau\lambda\kappa\eta}q_2^\kappa q^\tau \frac{-g^{\lambda\nu} + q^\lambda q^\nu/m_{\omega}^2}{q^2 - m_{\omega}^2}, \quad \text{(A18)}$$

$$\mathcal{M}_c^{D^0} = -i\frac{2gg_{DD\rho}g_{T^a_{c\bar{s}0}\rho D_s^*}}{f_0}\int \frac{d^4q}{(2\pi)^4} p_2^\mu \frac{-g^{\mu\nu} + q_1^\mu q_1^\nu/m_{D_s^{*+}}^2}{q_1^2 - m_{D_s^{*+}}^2} \times \frac{-g^{\nu\sigma} + q_2^\nu q_2^\sigma/m_{\rho^+}^2}{q_2^2 - m_{\rho^+}^2}(q_\sigma + p_{1\sigma})\frac{1}{q^2 - m_{D^0}^2}, \quad \text{(A19)}$$

$$\mathcal{M}_c^{D^{*0}} = i2g_{KD_s^*D^*}g_{D^*D\rho}g_{T^a_{c\bar{s}0}\rho D_s^*}\int\frac{d^4q}{(2\pi)^4}\epsilon_{\mu\nu\alpha\beta}q^\mu q_1^\alpha \times\frac{-g^{\beta\sigma}+q_1^\beta q_1^\sigma/m_{D_s^{*+}}^2}{q_1^2-m_{D_s^{*+}}^2}\frac{-g^{\sigma\eta}+q_2^\sigma q_2^\eta/m_{\rho^+}^2}{q_2^2-m_{\rho^+}^2} \times\epsilon_{\tau\eta\lambda\kappa}q_2^\tau(q^\lambda+p_1^\lambda)\frac{-g^{\nu\kappa}+q^\nu q^\kappa/m_{D^{*0}}^2}{q^2-m_{D^{*0}}^2}, \tag{A20}$$

$$\mathcal{M}_d^{K^0} = i\frac{\sqrt{2}gg_hg_{T^a_{c\bar{s}0}\rho D_s^*}}{f_0}\int\frac{d^4q}{(2\pi)^4}p_1^\mu \times\frac{-g^{\mu\nu}+q_1^\mu q_1^\nu/m_{D_s^{*+}}^2}{q_1^2-m_{D_s^{*+}}^2}\frac{-g^{\nu\eta}+q_2^\nu q_2^\eta/m_{\rho^+}^2}{q_2^2-m_{\rho^+}^2} \times(p_{2\eta}+q_\eta)\frac{1}{q^2-m_{K^0}^2}, \tag{A21}$$

$$\mathcal{M}_d^{K^{*0}} = i2g_{K^*D_s^*D}g_{K^*K\rho}g_{T^a_{c\bar{s}0}\rho D_s^*}\int\frac{d^4q}{(2\pi)^4}\epsilon_{\mu\nu\alpha\beta}q^\mu(q_1^\alpha+p_1^\alpha) \times\frac{-g^{\beta\sigma}+q_1^\beta q_1^\sigma/m_{D_s^{*+}}^2}{q_1^2-m_{D_s^{*+}}^2}\frac{-g^{\sigma\eta}+q_2^\sigma q_2^\eta/m_{\rho^+}^2}{q_2^2-m_{\rho^+}^2} \times\epsilon_{\tau\eta\lambda\kappa}q_2^\tau q^\lambda\frac{-g^{\nu\kappa}+q^\nu q^\kappa/m_{K^{*0}}^2}{q^2-m_{K^{*0}}^2}, \tag{A22}$$

where $m_{D_s^*}$, m_D, M_{D^*}, m_{K^*}, and m_K are the masses of the D_s^*, D, D^*, K^*, and K mesons, respectively. It is evident that these amplitudes suffer from ultraviolet (UV) divergence. Nevertheless, even the loops that are UV-finite receive contributions from short distances when integrated over the entire momentum space. To address this, we will utilize a UV regulator, as described in Ref. [56], which effectively suppresses the short-distance contributions, thereby rendering the amplitudes UV-finite. The UV regulator takes the form

$$\tilde{\Phi}(p_E^2/\Lambda^2) \equiv \exp(-p_E^2/\Lambda^2), \tag{A23}$$

where P_E is the Euclidean Jacobi momentum defined as $P_E = m_i p_j/(m_i+m_j) - m_j p_i(m_i+m_j)$ for the (ij) molecule.

Furthermore, we adopt the dipole form factor $\mathcal{F}(q^2) = (\Lambda^2-m^2)/(\Lambda^2-q^2)$ to account for the off-shell effect of the exchanged mesons. In this expression, m and q represent the mass and four-momentum of the exchanged mesons, respectively. The parameter Λ is typically parametrized as $\Lambda = m+\alpha\Lambda_{\rm QCD}$, where $\Lambda_{\rm QCD} = 220$ MeV. The value of α is chosen to be approximately 1.0 to ensure that Λ closely aligns with the mass of the exchanged mesons. In this study, we consider a range of α values within $0.91 \le \alpha \le 1.0$, a range derived from experimental data [57]. Then we have

$$\mathcal{M}_{\rm total} = \sum_{i=a,b,c,d}\mathcal{M}_i\tilde{\Phi}(p_E^2/\Lambda^2)\mathcal{F}^2(q^2). \tag{A24}$$

Once the amplitudes are determined, the corresponding partial decay widths can be obtained, which read

$$\Gamma(T^a_{c\bar{s}0}(2900)^{++}\to K^+D^+) = \frac{1}{8\pi}\frac{|\vec{p}_{K^+}|}{m^2_{T^a_{c\bar{s}0}(2900)^{++}}}\overline{|\mathcal{M}|^2}, \tag{A25}$$

where $\vec{p}_{K^+}$ is the three-momentum of the decay products in the center-of-mass frame, and the overline indicates the sum over the polarization vectors of the final hadrons.

[1] S. Godfrey and N. Isgur, Phys. Rev. D **32**, 189 (1985).
[2] R. Koniuk and N. Isgur, Phys. Rev. D **21**, 1868 (1980); **23**, 818(E) (1981).
[3] N. Isgur and G. Karl, Phys. Rev. D **19**, 2653 (1979); **23**, 817 (E) (1981).
[4] B. S. Zou and D. O. Riska, Phys. Rev. Lett. **95**, 072001 (2005).
[5] D. O. Riska and B. S. Zou, Phys. Lett. B **636**, 265 (2006).
[6] C. S. An, D. O. Riska, and B. S. Zou, Phys. Rev. C **73**, 035207 (2006).
[7] B. S. Zou, Nucl. Phys. **A835**, 199 (2010).
[8] B. S. Zou, Nucl. Phys. **A827**, 333C (2009).
[9] B. C. Liu and B. S. Zou, Phys. Rev. Lett. **96**, 042002 (2006).
[10] J. J. Xie, B. S. Zou, and H. C. Chiang, Phys. Rev. C **77**, 015206 (2008).
[11] S. K. Choi *et al.* (Belle Collaboration), Phys. Rev. Lett. **91**, 262001 (2003).
[12] R. Aaij *et al.* (LHCb Collaboration), Phys. Rev. Lett. **115**, 072001 (2015).
[13] R. Aaij *et al.* (LHCb Collaboration), Phys. Rev. Lett. **117**, 082002 (2016).
[14] R. Aaij *et al.* (LHCb Collaboration), Phys. Rev. Lett. **117**, 082003 (2016).
[15] R. Aaij *et al.* (LHCb Collaboration), Phys. Rev. Lett. **122**, 222001 (2019).
[16] R. Aaij *et al.* (LHCb Collaboration), Sci. Bull. **66**, 1278–1287 (2021).

[17] R. Aaij *et al.* (LHCb Collaboration), Phys. Rev. Lett. **131**, 031901 (2023).
[18] R. Aaij *et al.* (LHCb Collaboration), Phys. Rev. Lett. **131**, 041902 (2023).
[19] R. Molina, T. Branz, and E. Oset, Phys. Rev. D **82**, 014010 (2010).
[20] R. Chen and Q. Huang, arXiv:2208.10196.
[21] Z. L. Yue, C. J. Xiao, and D. Y. Chen, Phys. Rev. D **107**, 034018 (2023).
[22] S. S. Agaev, K. Azizi, and H. Sundu, Phys. Rev. D **107**, 094019 (2023).
[23] M. Y. Duan, M. L. Du, Z. H. Guo, E. Wang, and D. Y. Chen, arXiv:2307.04092.
[24] H. W. Ke, Y. F. Shi, X. H. Liu, and X. Q. Li, Phys. Rev. D **106**, 114032 (2022).
[25] F. X. Liu, R. H. Ni, X. H. Zhong, and Q. Zhao, Phys. Rev. D **107**, 096020 (2023).
[26] J. Wei, Y. H. Wang, C. S. An, and C. R. Deng, Phys. Rev. D **106**, 096023 (2022).
[27] X. S. Yang, Q. Xin, and Z. G. Wang, Int. J. Mod. Phys. A **38**, 2350056 (2023).
[28] D. K. Lian, W. Chen, H. X. Chen, L. Y. Dai, and T. G. Steele, arXiv:2302.01167.
[29] C. Jiang, Y. Jin, S. Y. Li, Y. R. Liu, and Z. G. Si, Symmetry **15**, 695 (2023).
[30] V. Dmitrašinović, arXiv:2301.05471.
[31] P. G. Ortega, D. R. Entem, F. Fernandez, and J. Segovia, arXiv:2305.14430.
[32] R. Molina and E. Oset, Phys. Rev. D **107**, 056015 (2023).
[33] Y. H. Ge, X. H. Liu, and H. W. Ke, Eur. Phys. J. C **82**, 955 (2022).
[34] V. Obraztsov (OKA Collaboration), Nucl. Part. Phys. Proc. **273–275**, 1330 (2016).
[35] B. Velghe (NA62-RK and NA48/2 Collaboration), Nucl. Part. Phys. Proc. **273–275**, 2720 (2016).
[36] C. Quintans (AMBER Collaboration), Few-Body Syst. **63**, 72 (2022).
[37] T. Nagae, Nucl. Phys. **A805**, 486 (2008).
[38] Y. Dong, A. Faessler, T. Gutsche, and V. E. Lyubovitskij, Phys. Rev. D **90**, 094001 (2014).
[39] H. Zhu and Y. Huang, Phys. Rev. D **100**, 054031 (2019).
[40] Y. Dong, A. Faessler, T. Gutsche, S. Kumano, and V. E. Lyubovitskij, Phys. Rev. D **82**, 034035 (2010).
[41] M. Y. Duan, E. Wang, and D. Y. Chen, arXiv:2305.09436.
[42] R. L. Workman *et al.* (Particle Data Group), Prog. Theor. Exp. Phys. **2022**, 083C01 (2022).
[43] J. He, Z. Ouyang, X. Liu, and X. Q. Li, Phys. Rev. D **84**, 114010 (2011).
[44] J. J. Xie, Y. B. Dong, and X. Cao, Phys. Rev. D **92**, 034029 (2015).
[45] P. Lebiedowicz and A. Szczurek, Phys. Rev. D **85**, 014026 (2012).
[46] P. Lebiedowicz, R. Pasechnik, and A. Szczurek, Phys. Lett. B **701**, 434 (2011).
[47] G. Pakhlova *et al.* (Belle Collaboration), Phys. Rev. D **77**, 011103 (2008).
[48] B. Aubert *et al.* (*BABAR* Collaboration), Phys. Rev. D **76**, 111105 (2007).
[49] X. D. Guo, D. Y. Chen, H. W. Ke, X. Liu, and X. Q. Li, Phys. Rev. D **93**, 054009 (2016).
[50] S. H. Kim, S. i. Nam, D. Jido, and H. C. Kim, Phys. Rev. D **96**, 014003 (2017).
[51] R. Casalbuoni, A. Deandrea, N. Di Bartolomeo, R. Gatto, F. Feruglio, and G. Nardulli, Phys. Rep. **281**, 145 (1997).
[52] M. Altenbuchinger, L. S. Geng, and W. Weise, Phys. Rev. D **89**, 014026 (2014).
[53] Y. s. Oh, T. Song, and S. H. Lee, Phys. Rev. C **63**, 034901 (2001).
[54] Z. w. Lin and C. M. Ko, Phys. Rev. C **62**, 034903 (2000).
[55] R. S. Azevedo and M. Nielsen, Phys. Rev. C **69**, 035201 (2004).
[56] Y. H. Lin, C. W. Shen, F. K. Guo, and B. S. Zou, Phys. Rev. D **95**, 114017 (2017).
[57] Y. Dong, A. Faessler, T. Gutsche, Q. Lü, and V. E. Lyubovitskij, Phys. Rev. D **96**, 074027 (2017).